ANTIOXIDANTS & REDOX SIGNALING
Volume 17, Number 3, 2012

DOI: 10.1089/ars.2011.4168

ORIGINAL RESEARCH COMMUNICATION

Extracellular Calcium-Sensing Receptor Is Critical in Hypoxic Pulmonary Vasoconstriction

Jiwei Zhang,[1,2,*] Juan Zhou,[1,2,*] Lei Cai,[1,2] Yankai Lu,[1,2] Tao Wang,[2] Liping Zhu,[1,2] and Qinghua Hu[1,2,3]

Abstract

Aims: The initiation of hypoxic pulmonary vasoconstriction (HPV) involves an increase in cytosolic calcium ($[Ca^{2+}]_i$) in pulmonary artery (PA) smooth muscle cells (PASMCs). Both the processes depend on extracellular Ca^{2+}. Extracellular Ca^{2+} can be sensed by extracellular calcium-sensing receptor (CaSR). This study aims at determining whether CaSR is pivotal in the initiation of HPV. ***Results:*** Experiments were performed in cultured PASMCs, isolated PAs, and rats including CaSR knockdown preparations. Both hypoxia and H_2O_2 equivalent to the level achieved by hypoxia increased $[Ca^{2+}]_i$ in an extracellular Ca^{2+}-dependent manner in PASMCs, and this was inhibited by CaSR knockdown or its negative allosteric modulator, Calhex231. Hypoxia-increased H_2O_2 generation was diminished by mitochondria depletion. Mitochondria depletion abolished hypoxia-induced $[Ca^{2+}]_i$ increase (HICI), which was reversed by H_2O_2 repletion. CaSR knockdown or Calhex231, however, prevented the reversible effect of H_2O_2. HICI was abolished by catalase-polyethylene glycol (PEG-Catalase), not superoxide dismutase-polyethylene glycol (PEG-SOD) pretreatment, attenuated by ryanodine receptor3-knockdown or inhibition of store-operated Ca^{2+} entry. HPV *in vitro* and *in vivo* was inhibited by Calhex231 and by CaSR knockdown. ***Innovation:*** A novel mechanism underlying HPV is revealed by the role of CaSR in orchestrating reactive oxygen species and $[Ca^{2+}]_i$ signaling. ***Conclusions:*** The activation of mitochondrial H_2O_2-sensitized CaSR by extracellular Ca^{2+} mediates HICI in PASMCs and, thus, initiates HPV. *Antioxid. Redox Signal*. 17, 471–484.

Introduction

HYPOXIC PULMONARY VASOCONSTRICTION (HPV) matches ventilation with perfusion and also leads to pulmonary hypertension. The initiation of HPV involves an increase in cytosolic calcium ($[Ca^{2+}]_i$) in pulmonary artery smooth muscle cells (PASMCs) (20, 33, 37, 38, 43). However, the signaling pathways for hypoxia-induced $[Ca^{2+}]_i$ increase (HICI) remains highly controversial (20, 33, 37, 38, 43).

Many previous studies have shown consistently that HICI and HPV were largely dependent on extracellular Ca^{2+} (9, 10, 13, 19, 25, 29, 34, 35, 42). Apparently, the extracellular Ca^{2+} dependence can be interpreted as the Ca^{2+} source for Ca^{2+} influx from extracellular space stimulated by hypoxia. Extracellular Ca^{2+} entry may be activated by hypoxia-altered level of reactive oxygen species (ROS) (1, 18, 26, 39, 41). The suggested Ca^{2+} entry pathways by hypoxia include store- (4, 23, 29, 35, 42) and voltage-operated Ca^{2+} influx (1, 20, 43). Meanwhile, Ca^{2+} release channel(s) especially ryanodine re-

Innovation

Hypoxic pulmonary vasoconstriction (HPV) matches lung ventilation with blood perfusion and also leads to pulmonary hypertension. The mechanism underlying HPV remains largely unknown. The Ca^{2+} sensitivity of calcium-sensing receptor (CaSR) in pulmonary artery smooth muscle cells is enhanced by mitochondria-derived reactive oxygen species (ROS) during hypoxia. The subsequent activation of sensitized CaSR by extracellular calcium then triggers intracellular calcium release mainly from ryanodine receptor and extracellular calcium influx primarily from store-operated calcium entry pathway. HPV *in vitro* and *in vivo* is inhibited by Calhex231 and by CaSR knockdown. The pivotal role of CaSR in orchestrating ROS and cytosolic calcium ($[Ca^{2+}]_i$) signaling is revealed as a new mechanism for the triggering of HPV, and the CaSR is also suggested as a novel target for the treatment of HPV-related diseases.

[1]Department of Pathophysiology, [2]Key Laboratory of Pulmonary Diseases of Ministry of Health, and [3]Key Laboratory of Environment and Health of Ministry of Education, Tongji Medical College, Huazhong University of Science and Technology (HUST), Wuhan, People's Republic of China.
*These authors contributed equally to this work.

ceptors (RyRs) have also been broadly documented to be involved in HICI and HPV (8, 12, 15, 32, 34, 48).

Extracellular Ca^{2+} is also the ligand for extracellular calcium-sensing receptor (CaSR) (14). The dependence of HICI and HPV on extracellular Ca^{2+} may not be understood solely as Ca^{2+} influx secondary to the depletion of intracellular Ca^{2+} stores by hypoxia. Substantial progress in this controversial point warrants a novel attempt to elucidate how these different Ca^{2+} pathways orchestrate to induce $[Ca^{2+}]_i$ elevation during hypoxia. As a matter of fact, however, it has never been studied whether extracellular Ca^{2+} plays any role(s) in addition to the source of Ca^{2+} influx from extracellular space in HICI and HPV.

CaSR is a G-protein-coupled membrane receptor that senses extracellular Ca^{2+} concentration and conveys this information to intracellular space through multiple signal pathways including $[Ca^{2+}]_i$ and extracellular regulated protein kinase (14). CaSR protein is expressed in vascular smooth muscle cells (6, 21, 45). The activation of CaSR in vascular smooth muscle cells increases $[Ca^{2+}]_i$ and induces a vasoconstriction of the gerbilline spiral modiolar artery (45). Additionally, functional CaSR appears sensitive to redox status (2, 47).

This study aimed at investigating the mechanism underlying extracellular Ca^{2+} dependence of HICI and its associations with RyR (8, 15, 34, 48), store-operated Ca^{2+} influx (SOC) (4, 23, 29, 35, 42), and HPV. It was found that functional CaSR, which can be sensitized by hypoxia-induced ROS, serves as a bridge between extracellular Ca^{2+} and $[Ca^{2+}]_i$ elevation and, therefore, is pivotal in HPV.

Results

Expression of a functional CaSR: sensing extracellular Ca^{2+}

Immunocytostaining showed the major localization of CaSR in the cytosol in permeabilized PASMCs and the membrane localization of the mature functional protein in nonpermeabilized PASMCs (Fig. 1A). Western blot on cell

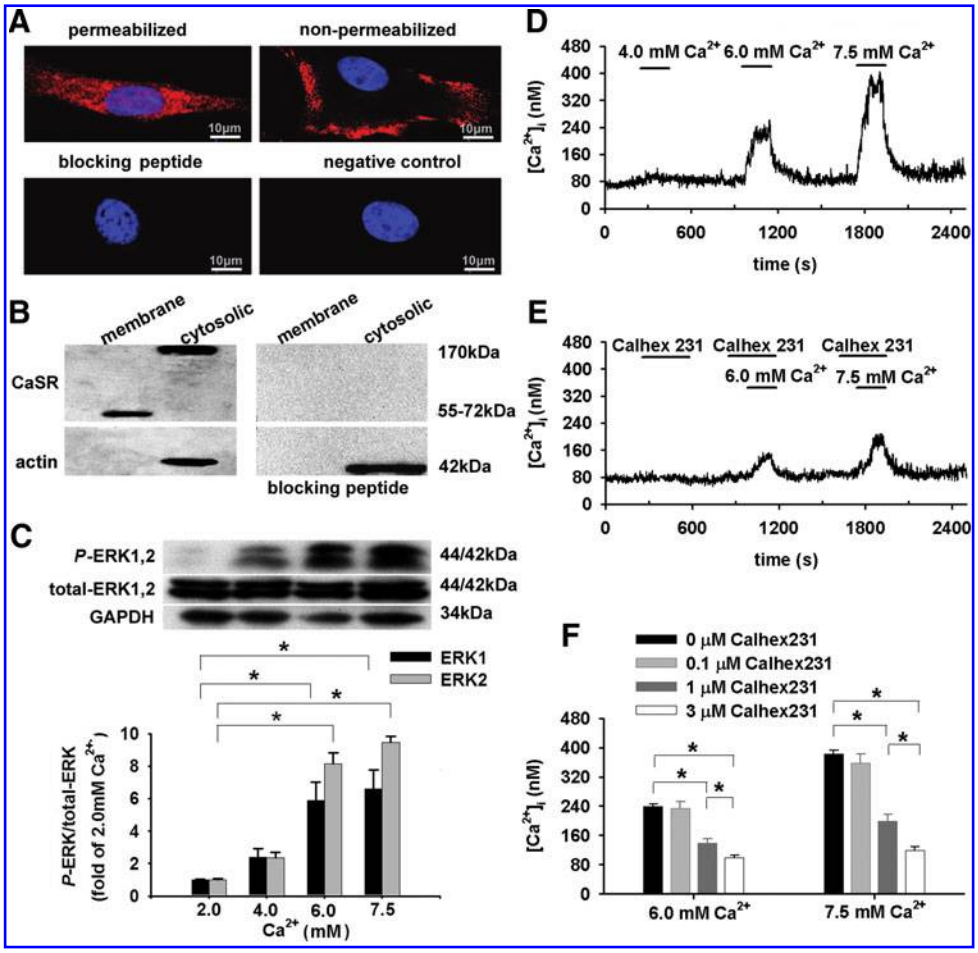

FIG. 1. Expression of a functional calcium-sensing receptor (CaSR) in pulmonary artery smooth muscle cells (PASMCs). **(A)** Indirect immunocytochemical staining of PASMCs in culture for CaSR (*red*) and nucleus (*blue*) in permeabilized (*upper left*) and nonpermeabilized preparations (*upper right*) as well as in the presence of a specific blocking peptide (*lower left*, nonpermeabilized preparations) and in a negative control without incubation of anti-CaSR antibody (*lower right*, nonpermeabilized preparations; $n=3$). **(B)** Western blot for CaSR in the absence (*left*) and presence (*right*) of a specific blocking peptide in cell lysate prepared from cytoplasm and membrane ($n=3$). **(C)** Enhanced phosphorylation of ERK1,2 in PASMCs in response to a 3 min stimulation of 4.0, 6.0, and 7.5 mM $[Ca^{2+}]_o$, respectively ($n=3$, $^*p<0.05$). **(D)** CaSR functional evaluation by cytosolic calcium ($[Ca^{2+}]_i$) monitoring in PASMCs in response to elevated $[Ca^{2+}]_o$ ($n=23$). **(E)** Inhibition of $[Ca^{2+}]_i$ response by 1 μM Calhex231 ($n=21$). **(F)** Dose-dependent inhibition of $[Ca^{2+}]_i$ response by Calhex231 ($^*p<0.05$).

lysate simultaneously isolated from cytoplasm and membrane revealed a 170 kDa band, presumably a prematured form (24, 50) and the other 55–72 kDa one, respectively (Fig. 1B).

To determine whether the CaSR protein is functional, PASMCs were exposed to increased extracellular Ca^{2+} concentration ($[Ca^{2+}]_o$) (5). A 3-min $[Ca^{2+}]_o$ elevation from 2.0 to 6.0 and 7.5 mM enhanced phosphorylation of ERK1,2 (p44/p42; Fig. 1C), an indication of CaSR activation (14) and increased $[Ca^{2+}]_i$ ($n=23$, $p<0.05$ for each, Fig. 1D, F). (1S,2S,1′R)-N1-(4-chlorobenzoyl)-N2-[1-(1-naphthyl)ethyl]-1,2-diaminocyclo-hexane (Calhex231), the negative allosteric modulator of CaSR, dose-dependently inhibited $[Ca^{2+}]_o$ elevation-stimulated $[Ca^{2+}]_i$ increase ($p<0.05$, Fig. 1E, F). Thus, PASMCs can sense $[Ca^{2+}]_o$ through CaSR-mediated $[Ca^{2+}]_i$ signaling.

HICI: extracellular Ca^{2+} dependence, Calhex231 inhibition, and CaSR dependence

Hypoxia, by a quick superfusion of PASMCs with hypoxic medium for 3 min, increased $[Ca^{2+}]_i$ ($n=51$, $p<0.01$, Fig. 2A, C). The HICI was completely abolished or significantly inhibited by the removal of extracellular Ca^{2+} ($n=43$, Fig. 2B, C), the presence of Calhex231 ($n=8$, Fig. 2D, E), or CaSR knockdown ($p<0.01$ *vs.* blank or nonspecific shRNA respectively, Fig. 3C–F). Of note, CaSR knockdown abolished/inhibited $[Ca^{2+}]_i$ response to 6.0 and 7.5 mM $[Ca^{2+}]_o$, whereas it does not affect the store Ca^{2+} contents in PASMCs (Supplementary Figs. S1 and S2; Supplementary Data are available online at www.liebertonline.com/ars). Thus, HICI depends on extracellular Ca^{2+}-associated CaSR activation or a permissive role of CaSR.

Ca^{2+} sensitivity of CaSR: enhanced by ROS

Hypoxia, as indicated by a quick decline in PO_2 from 154 ± 4 to 19 ± 1 mmHg ($n=4$), stimulated an abrupt increase in ROS ($n=22$, Fig. 4Ai), estimated (30) to a level equivalent to 15.6 μM extracellular H_2O_2 ($n=21$–26 for each dose, Fig. 4Aii). The hypoxia-stimulated ROS generation in PASMCs was confirmed using a redox-sensitive green fluorescent protein (GFP)-RoGFP (Fig. 4Aiii) (40). Hypoxia-stimulated ROS generation is not affected by Calhex231 (Supplementary Fig. S3). About 15.6 μM H_2O_2, not a lower concentration of 13.0 μM (Supplementary Fig. S4), which did not induce any $[Ca^{2+}]_i$ transient in the absence of extracellular Ca^{2+}, triggered a $[Ca^{2+}]_i$ transient in the presence of 2 mM $[Ca^{2+}]_o$ ($n=5$, Fig. 4Bi, Biii). These results are consistent with previous studies showing that H_2O_2 increased $[Ca^{2+}]_i$ in smooth muscle cells (18, 46), and the $[Ca^{2+}]_i$ increase by low μM H_2O_2 depended

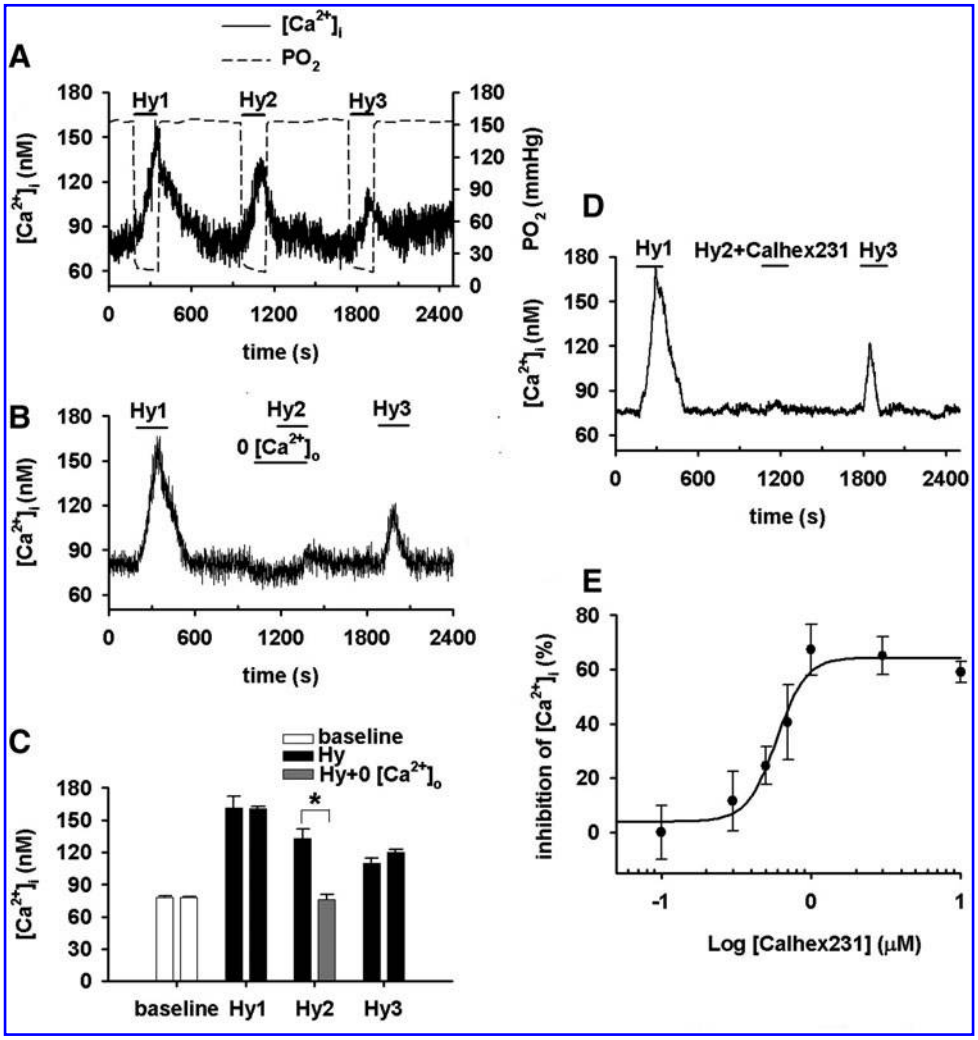

FIG. 2. Extracellular Ca^{2+} dependence of hypoxia-induced $[Ca^{2+}]_i$ increase and inhibition by Calhex231. (A) Representative curve of $[Ca^{2+}]_i$ responses to three repetitive episodes of hypoxia (Hy1, Hy2, and Hy3) each for 3 min in the presence of 2.0 mM extracellular Ca^{2+} ($n=51$). **(B)** Representative curve of $[Ca^{2+}]_i$ responses to repetitive episodes of hypoxia in the presence (Hy1 and Hy3) or absence (Hy2) of 2.0 mM extracellular Ca^{2+} ($n=43$). **(C)** Averaged $[Ca^{2+}]_i$ levels at baseline and hypoxic episodes (*$p<0.05$). **(D)** Representative curve of $[Ca^{2+}]_i$ responses to repetitive episodes of hypoxia in the absence (Hy1 and Hy3) and presence (Hy2) of 1 μM Calhex231 ($n=8$). **(E)** Dose-dependent inhibition of $[Ca^{2+}]_i$ peak response to hypoxia by Calhex231 (four parameter logistic regression, $p<0.05$, $n=8$ for each dose).

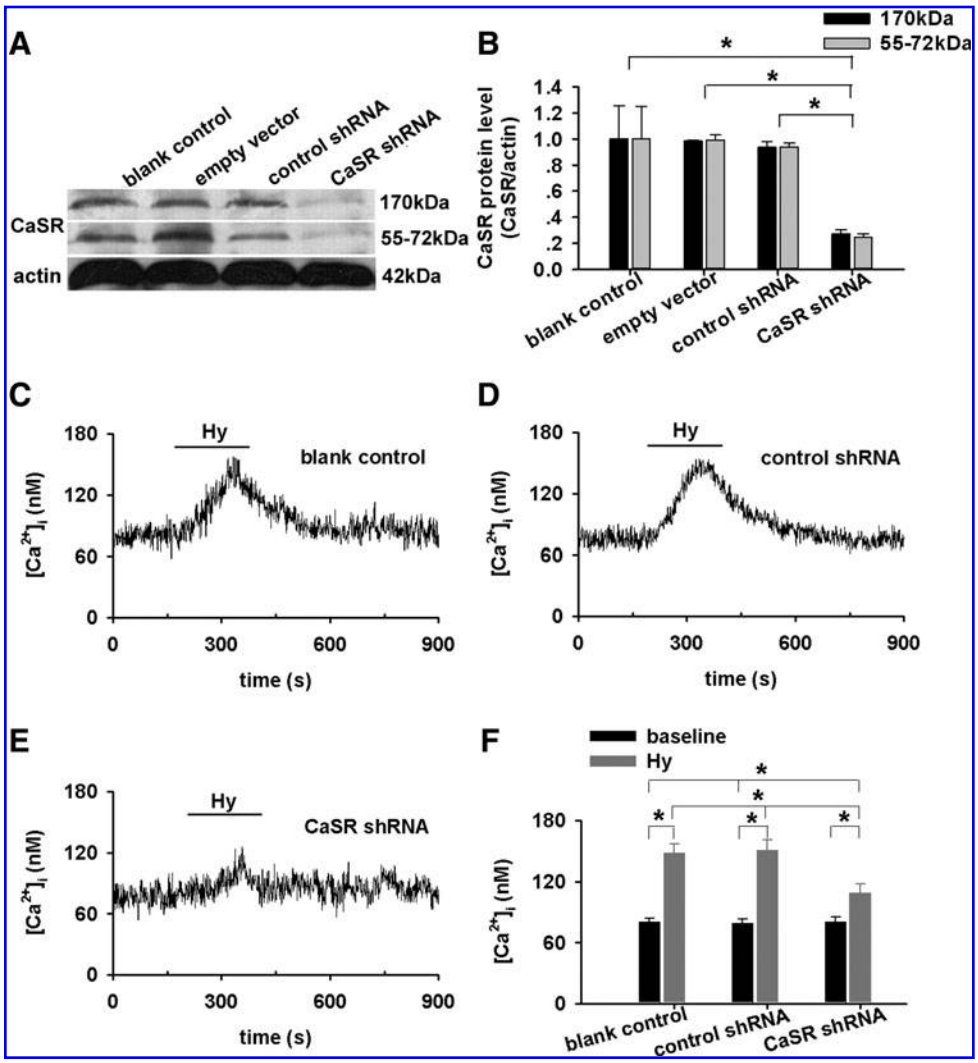

FIG. 3. CaSR dependence of hypoxia-induced $[Ca^{2+}]_i$ increase. (A) Western blot showing shRNA-mediated CaSR knockdown. **(B)** Averaged densitometry in control and CaSR shRNA-treated PASMCs (*$p<0.05$, $n=3$ for each). **(C–E)** Representative curve of $[Ca^{2+}]_i$ responses to hypoxia (Hy) in blank control ($n=11$, **C**), control shRNA ($n=14$, **D**) and CaSR specific shRNA-treated PASMCs ($n=9$, **E**) in the presence of 2.0 mM extracellular Ca^{2+}. **(F)** Averaged $[Ca^{2+}]_i$ peaks in response to hypoxia (*$p<0.05$).

on extracellular Ca^{2+} (46). 1 μM Calhex231 and CaSR-knockdown significantly inhibited 15.6 μM H_2O_2-induced $[Ca^{2+}]_i$ transient ($n=13$, Fig. 4Bii, Biii, C). $[Ca^{2+}]_o$ elevation-induced $[Ca^{2+}]_i$ signal in PASMCs is enhanced by the concomitant presence of 15.6 μM H_2O_2 or under hypoxia (Supplementary Fig. S5). Thus, the Ca^{2+} sensitivity of CaSR in inducing a $[Ca^{2+}]_i$ transient can be enhanced by ROS at the level achieved by hypoxia in PASMCs.

CaSR-dependent $[Ca^{2+}]_i$ increase by hypoxia: role of mitochondria-derived H_2O_2

Mitochondria depletion (7, 39) using ethidium bromide almost completely diminished ROS generation by hypoxia ($n=27$, $p<0.01$ *vs.* control with or without pyruvate (Py) and uridine (Ur), Fig. 5A). Hypoxia triggered similar $[Ca^{2+}]_i$ increase in control PASMCs cultured in the presence ($n=8$, $p<0.01$, Fig. 5Bi, Bv) and absence of Py and Ur (Fig. 2A). Mitochondria depletion completely abolished HICI, and this was reversed by exposure of PASMCs to 15.6 μM H_2O_2 (Fig. 5Bii, Bv). The exposure of H_2O_2-reversed $[Ca^{2+}]_i$ increase during hypoxia in mitochondria-depleted PASMCs was prevented by 1 μM Calhex231 ($n=15$, $p<0.01$ *vs.* co-exposure of H_2O_2 in the absence of Calhex231, Fig. 5Biii, Bv) and by CaSR knockdown (Fig. 5Biv, Bv), suggesting that mitochondria-derived ROS sensitizes CaSR and thereafter triggers HICI.

PEG-Catalase, not PEG-SOD loaded into PASMCs (7), abolished HICI (Fig. 5Ci–Ciii), clarifying the specific role of intracellular H_2O_2 in HICI.

HICI: RyR and SOC dependence

To determine the downstream target of CaSR activation by hypoxia, we manipulated the intracellular Ca^{2+} release and SOC pathways. The inhibition of RyR by 100 μM ryanodine, but not the inhibition of IP_3 receptor by 20 μM XeC, significantly attenuated HICI ($p<0.05$ *vs.* control, Fig. 6Ai, Aiv for ryanodine; $p=$nonsignificance *vs.* control, Fig. 6Aii, Aiv for XeC). These are consistent with previous studies using either genetically manipulated PASMCs (48) or pharmacological inhibitors (8, 11, 15, 34). Being accordant with other investigators (4, 23, 35), SOC inhibitor, 50 μM SKF96365 significantly inhibited HICI ($p<0.05$ *vs.* control, Fig. 6Aiii, Aiv). Similarly, Ryanodine and SKF96365, not XeC, inhibited H_2O_2-induced $[Ca^{2+}]_i$ increase (Fig. 6B, C).

RyR3 (48) and STIM1 knockdown block or profoundly inhibited hypoxia- and H_2O_2-induced $[Ca^{2+}]_i$ increase, respectively (Fig. 6D), revealing that RyR3 and STIM1 can be the

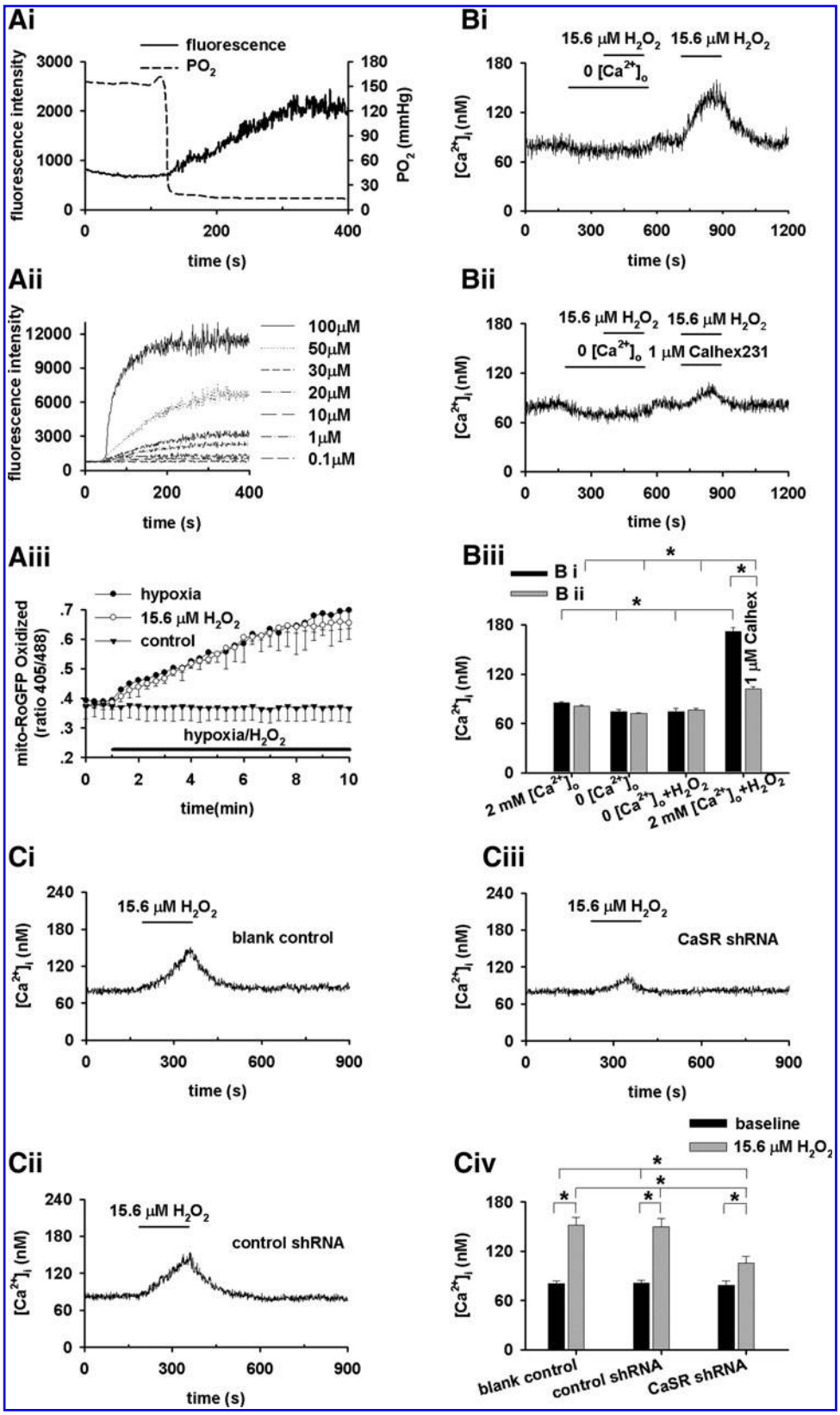

FIG. 4. Enhancement of Ca^{2+} sensitivity of CaSR by reactive oxygen species (ROS). (A) Hypoxia-triggered ROS generation in PASMCs was estimated by DCFDA. Representative curves of DCFDA fluorescence in PASMCs in response to hypoxia ($n=22$, **Ai**) and to a series of extracellular application of H_2O_2 ($n=21$–26, **Aii**). Averaged time-course alterations of ratios of mito-RoGFP fluorescence intensity from excitation at 405 and 488 nm and emission at 515 nm from PASMCs on exposure to hypoxia, 15.6 (μM H_2O_2, or normoxic control ($n=3$ for each, **Aiii**). **(B)** Representative curve of $[Ca^{2+}]_i$ in PASMCs in response to 15.6 μM H_2O_2 in the absence and then presence of 2.0 mM $[Ca^{2+}]_o$ ($n=5$, **Bi**); representative curve of $[Ca^{2+}]_i$ in PASMCs in response to 15.6 μM H_2O_2 in the absence and then co-presence of 2.0 mM $[Ca^{2+}]_o$ and 1 μM Calhex231 ($n=13$, **Bii**); averaged $[Ca^{2+}]_i$ baseline and peak responses to 15.6 μM H_2O_2 ($^*p<0.05$, **Biii**). **(C)** CaSR-mediated $[Ca^{2+}]_i$ response to 15.6 μM H_2O_2. Representative curves of $[Ca^{2+}]_i$ in response to 15.6 μM H_2O_2 in the presence of 2.0 mM $[Ca^{2+}]_o$ in control PASMCs ($n=12$, **Ci**), PASMCs treated with nonspecific- ($n=8$, **Cii**) and CaSR-specific shRNA ($n=7$, **Ciii**). Averaged $[Ca^{2+}]_i$ baseline and peak responses to 15.6 μM H_2O_2 ($^*p<0.05$, **Civ**).

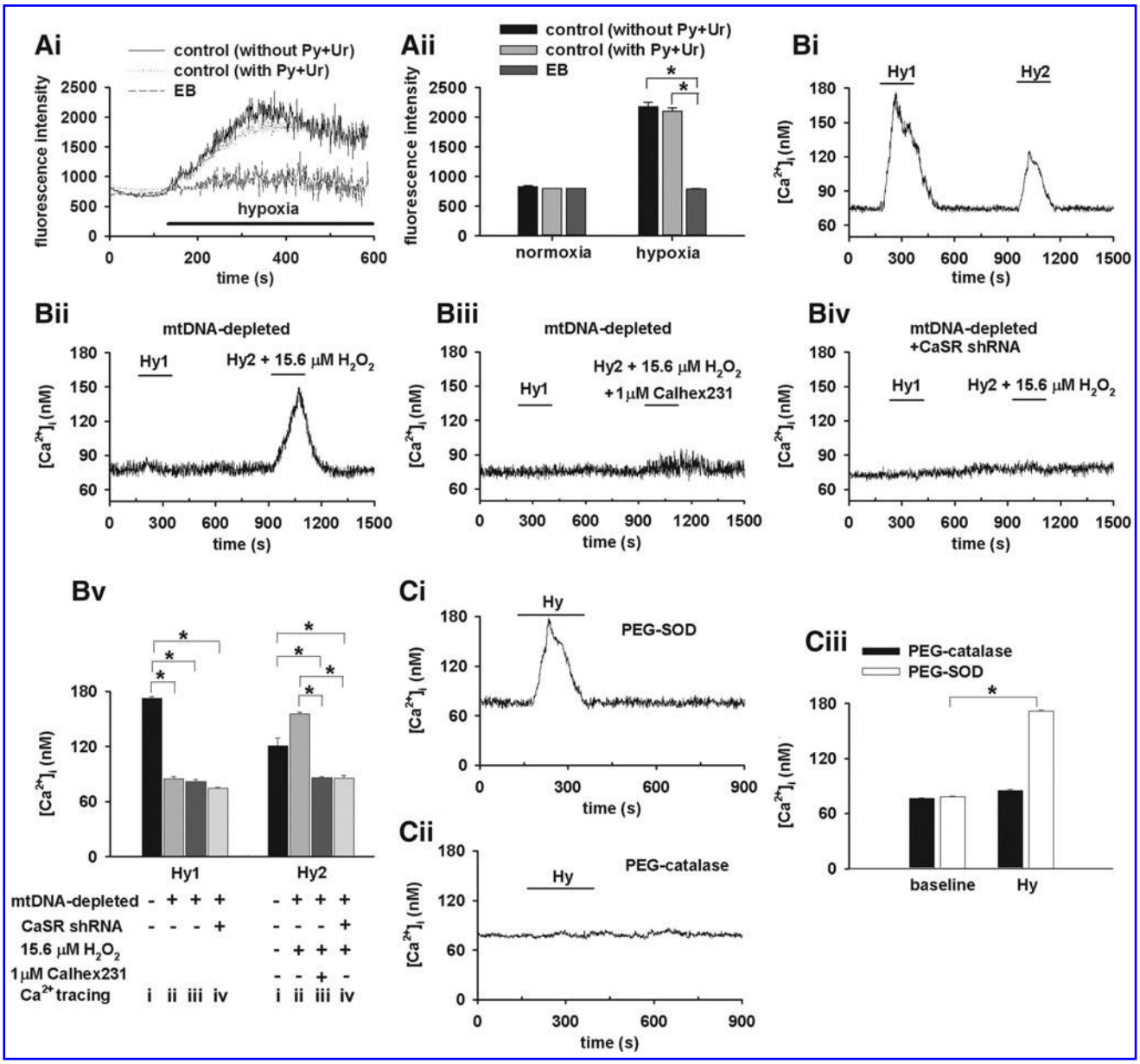

FIG. 5. Mitochondria-derived H_2O_2 in CaSR-mediated $[Ca^{2+}]_i$ increase by hypoxia. (A) Representative curves of DCFDA fluorescence in response to hypoxia in control PASMCs in the absence ($n=19$) or presence of pyruvate (Py) and uridine (Ur; $n=10$) and in mitochondria-depleted PASMCs ($n=26$, **Ai**). Averaged DCFDA fluorescence intensity (*$p<0.01$ *vs.* control PASMCs in the presence or absence of Py and Ur, **Aii**). **(B)** Representative curve of $[Ca^{2+}]_i$ responses to two repetitive episodes of hypoxia (Hy1 and Hy2) in PASMCs cultured with Py and Ur ($n=8$, **Bi**), to hypoxia in the absence (Hy1) and presence of 15.6 μM H_2O_2 (Hy2) in mtDNA-depleted PASMCs ($n=13$, **Bii**), to hypoxia in the absence (Hy1) and co-presence of 15.6 μM H_2O_2 and 1 μM Calhex231 (Hy2) in mtDNA-depleted PASMCs ($n=15$, **Biii**), to hypoxia in the absence (Hy1) and presence of 15.6 μM H_2O_2 (Hy2) in mtDNA-depleted PASMCs with CaSR knockdown ($n=13$, **Biv**). Averaged $[Ca^{2+}]_i$ peak responses to hypoxia (*$p<0.05$, **Bv**). **(C)** Representative curve of $[Ca^{2+}]_i$ responses to hypoxia in the PEG-SOD ($n=16$, **Ci**) and PEG-catalase ($n=15$, **Cii**)-pretreated PASMCs. PASMCs were pretreated overnight with 1000 U/ml PEG-SOD or 5000 U/ml PEG-catalase. Averaged $[Ca^{2+}]_i$ baseline and peak responses to hypoxia (*$p<0.05$, **Ciii**). Extracellular Ca^{2+} is 2.0 mM for all.

major molecular targets of CaSR activation or sensitization upon hypoxia and H_2O_2 stimulation. However, this study does not exclude the involvement of voltage-sensitive pathways (1, 25, 43), as verapamil also inhibited H_2O_2-induced $[Ca^{2+}]_i$ elevation ($n=12$, $p<0.05$ *vs.* control, Fig. 6C).

Under normal or normoxic conditions, CaSR activation (by elevating $[Ca^{2+}]_o$ to 6.0 mM) -induced $[Ca^{2+}]_i$ signal in PASMCs was inhibited by XeC (Fig. 7A–D), indicating that CaSR activation-induced $[Ca^{2+}]_i$ signal is mediated by IP_3 receptor, the well-established downstream target of CaSR (14). However, the downstream target turns to be RyR under hypoxic condition in PASMCs (Fig. 6). To reveal the discrepancy, the role of protein kinase A (PKA) pathway was explored. XeC did (Fig. 7F, H), whereas ryanodine failed to

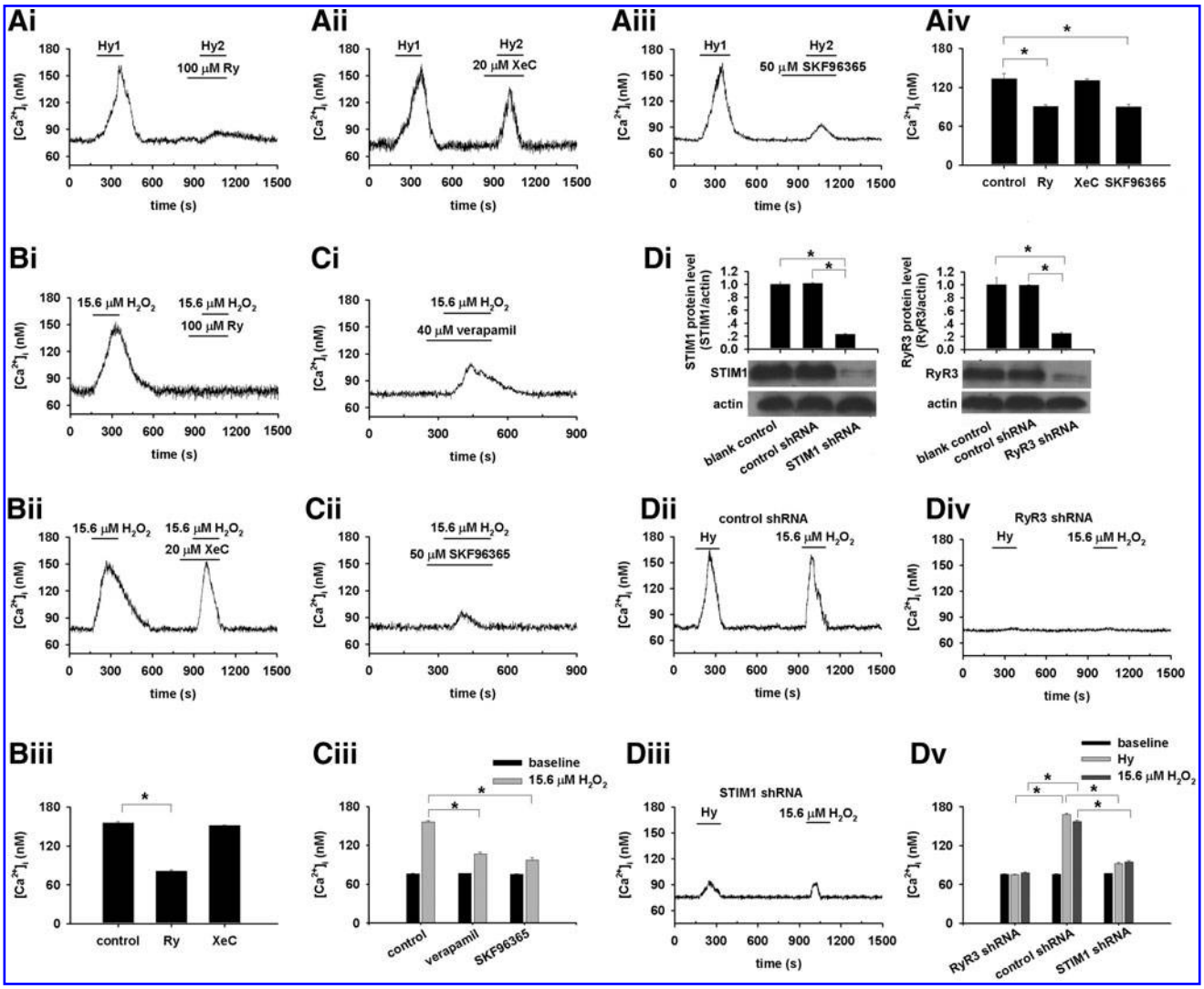

FIG. 6. Inhibition of hypoxia- and H_2O_2-induced $[Ca^{2+}]_i$ increase by manipulations of intracellular Ca^{2+} release and extracellular Ca^{2+} influx. (A) Representative curve of $[Ca^{2+}]_i$ responses to hypoxia alone (Hy1) and the second episode of hypoxia (Hy2) in the presence of ryanodine ($n=10$, **Ai**), XeC ($n=17$, **Aii**) or SKF96365 ($n=8$, **Aiii**). Averaged $[Ca^{2+}]_i$ peak responses to the second episode of hypoxia (*$p<0.05$, **Aiv**). **(B)** Representative curve of $[Ca^{2+}]_i$ responses to 15.6 μM H_2O_2 in the absence and the subsequent presence of ryanodine ($n=15$, **Bi**) or XeC ($n=17$, **Bii**). Averaged $[Ca^{2+}]_i$ peak responses to H_2O_2 (*$p<0.05$, **Biii**). **(C)** Representative curve of $[Ca^{2+}]_i$ responses to 15.6 μM H_2O_2 in the presence of verapamil ($n=12$, **Ci**) or SKF96365 ($n=17$, **Cii**). Averaged $[Ca^{2+}]_i$ peak responses to 15.6 μM H_2O_2 (*$p<0.05$, **Ciii**). **(D)** Western blotting and densimetric analysis of STIM1 (**Di**, *left*) and RyR3 (**Di**, *right*) level in control and shRNA-treated PASMCs ($n=3$ for each, *$p<0.01$, **Di**). Representative curve of $[Ca^{2+}]_i$ responses to hypoxia and 15.6 μM H_2O_2 in control ($n=6$, **Dii**), STIM1 knockdown ($n=9$, **Diii**), or RyR3 knockdown PASMCs ($n=24$, **Div**). Averaged $[Ca^{2+}]_i$ peak responses to hypoxia or H_2O_2 (*$p<0.05$, **Dv**). Extracellular Ca^{2+} is 2.0 mM for all.

(Fig. 7G, H), inhibit HICI in the presence of H-89, a PKA inhibitor, indicating that IP_3 receptor mediates HICI, while PKA signaling pathway is blocked. On the contrary, ryanodine did, whereas XeC failed to, inhibit HICI in the absence of H-89 (Fig. 7I–L), implying that rynodine receptor mediates HICI, while PKA signaling pathway is not blocked.

HPV: role of CaSR in vitro *and* in vivo

Phenylephrine (PE)-preconstricted PA rings showed no response to acetylcholine confirming the removal of endothelium; however, they contracted when each hypoxic challenge was applied to the vessels (Fig. 8Ai). Calhex231 dose-dependently inhibited the hypoxia-induced constriction of the vessel (four parameter logistic regression, $p<0.05$, Fig. 8Aiv). 15.6 μM H_2O_2 contracted rings in a way similar to hypoxia (Fig. 8Bi) that was also inhibited by 1 μM Calhex231 ($n=5$, $p<0.01$, Fig. 8Bii, Biii), suggesting the mechanistic role of H_2O_2 in sensing CaSR and the subsequent constriction of PA by hypoxia. Furthermore, the hypoxia-induced constriction of PA isolated from CaSR knockdown rats was profoundly inhibited as compared with control ($n=3$, $p<0.01$, Fig. 8C).

The 10 min episodes of hypoxia successively triggered typical HPV in rats ($n=4$, Fig. 9Ai), which was dose-dependently inhibited by Calhex231 (four-parameter logistic

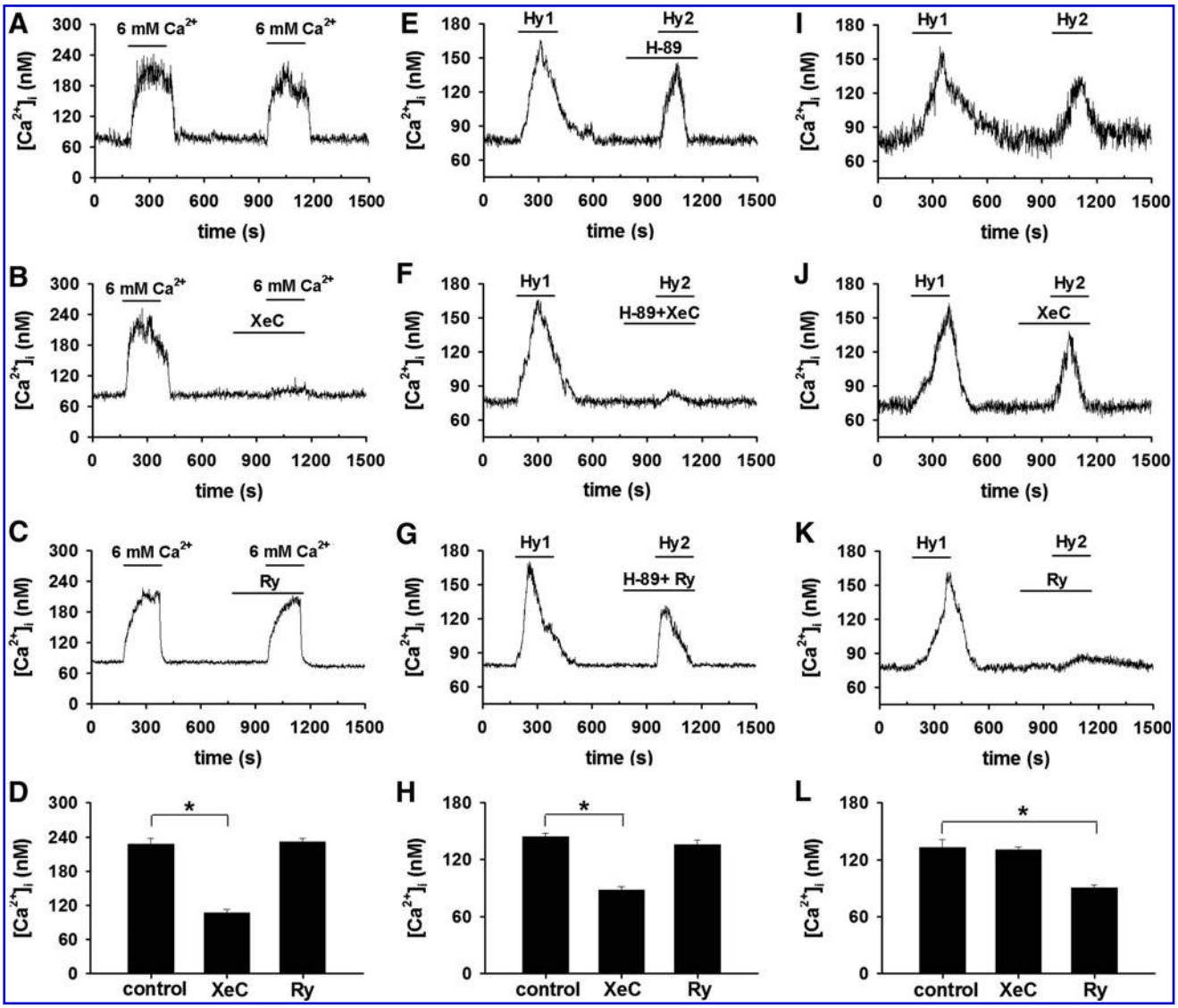

FIG. 7. The effect of protein kinase A (PKA) inhibition on CaSR-mediated $[Ca^{2+}]_i$ signal in PASMCs. (A) Representative tracing of $[Ca^{2+}]_i$ in PASMCs in response to repetitive elevation of $[Ca^{2+}]_o$ from 2.0 to 6.0 mM ($n = 11$). **(B)** Effect of 20 μM XeC on $[Ca^{2+}]_o$ elevation-induced $[Ca^{2+}]_i$ response ($n = 11$). **(C)**. Effect of 100 (μM ryanodine (Ry) on $[Ca^{2+}]_o$ elevation-induced $[Ca^{2+}]_i$ response ($n = 10$). **(D)** Averaged $[Ca^{2+}]_i$ responses in **A–C** ($^*p < 0.05$). **(E)** Representative tracing of $[Ca^{2+}]_i$ in PASMCs in response to hypoxia in the absence and then presence of 10 (μM H-89, a PKA inhibitor ($n = 6$). **(F)** Effect of XeC on hypoxia-induced $[Ca^{2+}]_i$ response in the presence of 10 (μM H-89 ($n = 8$). **(G)** Effect of ryanodine on hypoxia-induced $[Ca^{2+}]_i$ response in the presence of 10 (μM H-89 ($n = 10$). **(H)** Averaged $[Ca^{2+}]_i$ responses in **E–G** ($^*p < 0.05$). **(I)** Representative tracing of $[Ca^{2+}]_i$ in PASMCs in response to repetitive episodes of hypoxia ($n = 51$). **(J)** Effect of XeC on hypoxia-induced $[Ca^{2+}]_i$ response ($n = 17$). **(K)** Effect of ryanodine on hypoxia-induced $[Ca^{2+}]_i$ response ($n = 10$). **(L)** Averaged $[Ca^{2+}]_i$ responses in **I–K** ($^*p < 0.05$). For comparison, some results in Figures 2**A** and 6**A** were included here as **I–L**.

regression, $p < 0.05$, Fig. 9Aiv). HPV was found to be typical in control rats treated with nonspecific shRNA ($n = 3$, Fig. 9Bi), whereas significantly inhibited in CaSR knockdown rats ($n = 4$, $p < 0.01$ *vs.* control, Fig. 9Bii, Biii). CaSR knockdown did not affect PE-induced pulmonary vascular constriction in rats (not shown) or plasma Ca^{2+} level (Supplementary Fig. S6).

Discussion

The basal function of CaSR in PASMCs was first evaluated by elevating the extracellular Ca^{2+} to supraphysiological levels, the direct stimulus of CaSR (14) (Fig. 1). In the subsequent experiments revealing the actual role of CaSR in HPV, the extracellular Ca^{2+} was maintained at a physiological level.

Hypoxia induces an $[Ca^{2+}]_i$ increase (HICI) in PASMCs that depends on extracellular Ca^{2+} (Fig. 2). These results are broadly consistent with most of the previous observations well documented in literature including those on isolated or cultured PASMCs (9, 25, 34, 35), isolated pulmonary arteries (PAs) (13, 19, 29), and perfused lung or lung slices (10, 42). In the absence of extracellular Ca^{2+}, however, hypoxia was reported to cause a small and transient increase followed by a sustained decrease in $[Ca^{2+}]_i$ below baseline in canine PASMCs (22, 23), a small increase in rat PASMCs (25) or

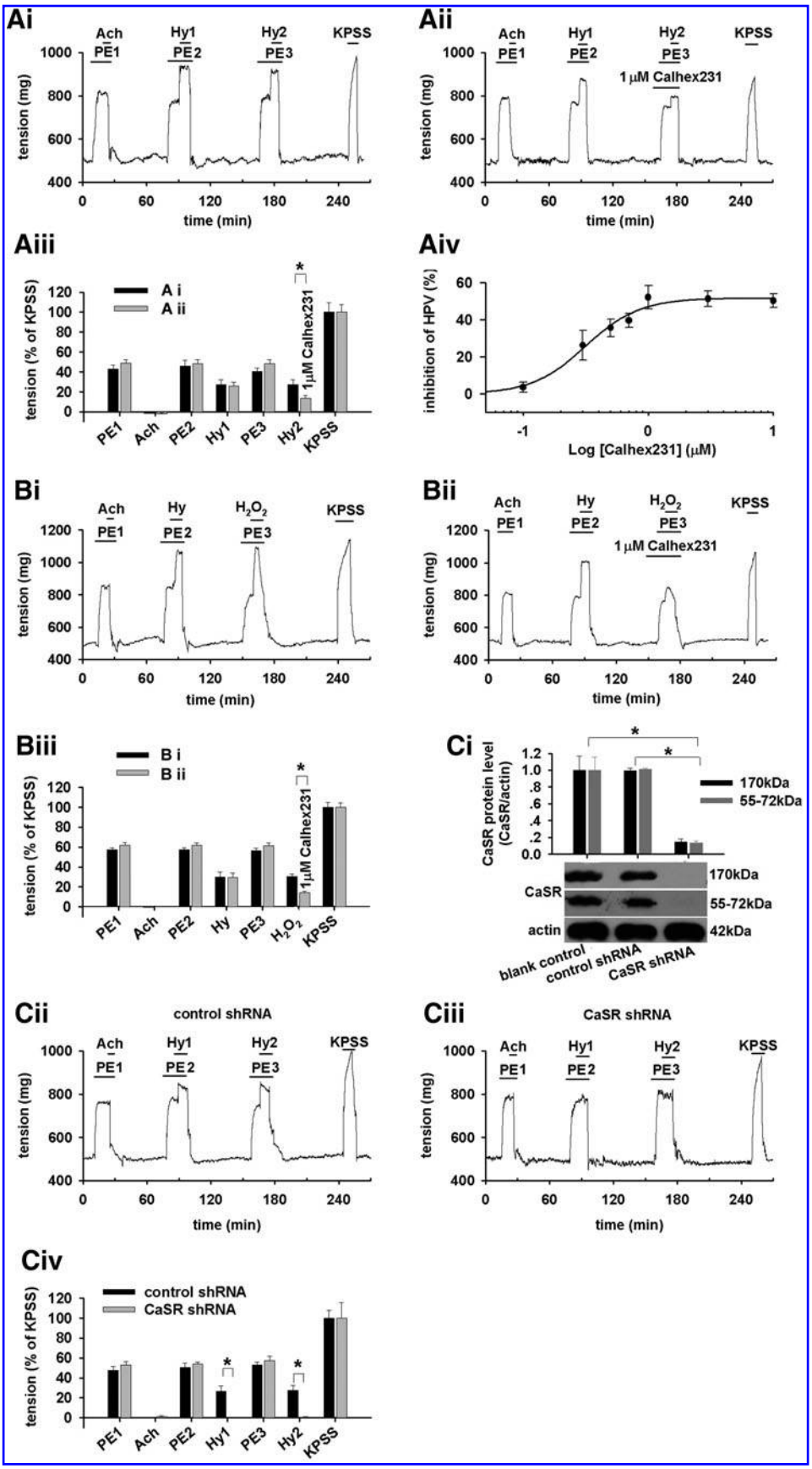

FIG. 8. Inhibition of hypoxic pulmonary vasoconstriction (HPV) and H_2O_2-induced pulmonary artery constriction *in vitro* by Calhex231 and CaSR knockdown. (A) Isometric tension of endothelium-removed pulmonary artery (PA) rings in response to acetylcholine (Ach) and two episodes of hypoxia (Hy1 and Hy2) sequentially each after preconstriction by phenylephrine (PE) and to a final exposure of 80 mM K^+ (KCl-physiological salt solution (KPSS), an equimolar substitution of K^+ for Na^+; $n=3$, **Ai**). Isometric tension of endothelium-removed PA in response to Ach and two episodes of hypoxia in the absence (Hy1) and presence of 1 μM Calhex231 (Hy2, $n=3$, **Aii**). Averaged responses to PE, Ach, and hypoxia as well as the effect of 1 μM Calhex231 (normalized to tension induced by KPSS, $^*p<0.01$, $n=3$, **Aiii**). Dose-dependent inhibition of HPV *in vitro* by Calhex231 (four parameter logistic regression, $p<0.05$, **Aiv**). **(B)** Isometric tension of endothelium-removed PA in response to Ach, hypoxia, and 15.6 μM H_2O_2 in the absence ($n=6$, **Bi**) and presence of 1 μM Calhex231 ($n=5$, **Bii**). Averaged responses to PE, Ach, hypoxia, and H_2O_2 as well as the effect of 1 μM Calhex231 ($^*p<0.01$, **Biii**). **(C)** Western blotting and densimetric analysis of CaSR level in endothelium-removed PA isolated from rats treated with shRNA ($n=4$, $^*p<0.01$, **Ci**). Isometric tension in response to Ach, hypoxia in endothelium-removed PA isolated from control ($n=5$, **Cii**), and CaSR shRNA-treated rats ($n=5$, **Ciii**). Averaged responses to PE, Ach, and hypoxia ($^*p<0.01$, **Civ**). The maximum constriction response to KPSS was used to normalize the tension for each experiment.

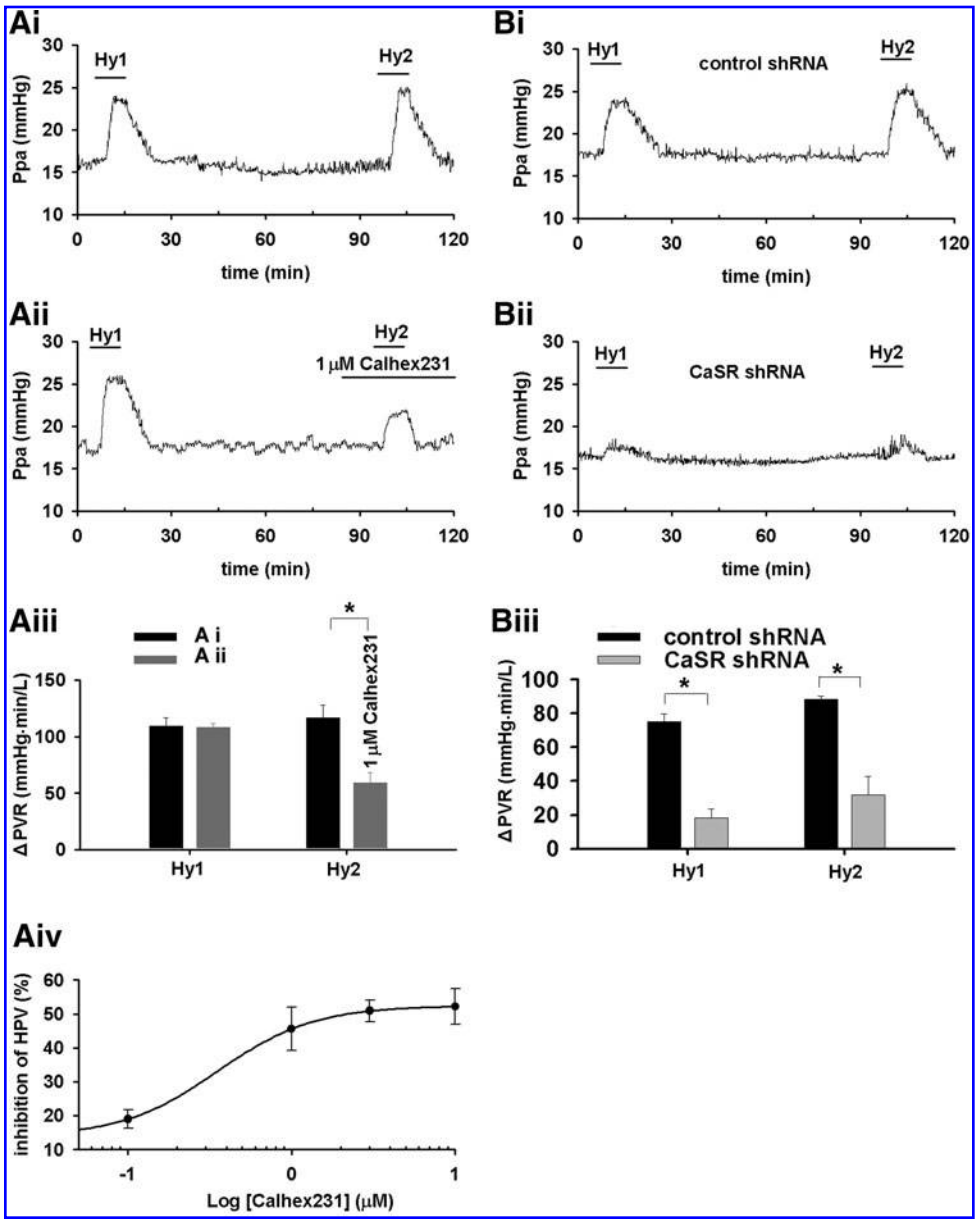

FIG. 9. Inhibition of HPV *in vivo* by Calhex231 and CaSR knockdown. (A) Pressure of pulmonary artery (Ppa) in response to successive episodes of hypoxia in the absence ($n=3$, **Ai**) and presence of 1 μM Calhex231 ($n=3$, **Aii**). Averaged increase in pulmonary vascular resistance (ΔPVR $^*p<0.01$, **Aiii**). Dose-dependent inhibition of HPV *in vivo* by Calhex231 (four parameter logistic regression, $p<0.05$, **Aiv**). **(B)** Ppa in response to successive episodes of hypoxia in control ($n=3$, **Bi**) and CaSR shRNA-treated rats ($n=4$, **Bii**). Averaged alterations of ΔPVR ($^*p<0.01$, **Biii**). The pulmonary vascular resistance (PVR) was calculated by Ppa-left ventricular end-diastolic pressure (LVEDP)/cardiac output (CO; $mmHg \cdot min \cdot L^{-1}$) and used to determine HPV as $\Delta PVR = PVR_{10\% O_2} - PVR_{20\% O_2} / PVR_{20\% O2}$ (%).

transient(s) in 34% of rat PASMCs examined (27). A transient contraction of rat PA rings by hypoxia in Ca^{2+}-free medium was also noted (12). This discrepancy can be due to differences in experimental preparations (3, 32) and heterogeneity of $[Ca^{2+}]_i$ response to hypoxia in PASMCs (27). Extracellular Ca^{2+} was shown to differentially affect hypoxic vasoconstriction in different species (32), and hypoxia also differentially affected $[Ca^{2+}]_i$ in PASMCs isolated from different regions of PA tree (3). Additional and potential reasons can be the spontaneous Ca^{2+} release in the absence of extracellular Ca^{2+} reported in a variety of cell types including vascular smooth muscle cells (31, 44) and endogenous peroxidase activity. Generally, the extracellular Ca^{2+} dependence of HICI was understood as the importance of Ca^{2+} influx in all previous studies. The present study, however, showed further that both Calhex231 and CaSR knockdown inhibited HICI in PASMCs (Figs. 2 and 3). This provides, to the best of our knowledge, the first clue of the CaSR involvement in HICI and HPV. These novel findings further imply that the extracellular Ca^{2+} dependence of HICI cannot be simply or merely interpreted as the resource of Ca^{2+} influx as presumed. An additional role of extracellular Ca^{2+}, the ligand of CaSR can be an initial trigger for the activation of CaSR during hypoxia and the subsequent $[Ca^{2+}]_i$ elevation and constriction.

The actual role of ROS in HPV remains controversial, and even both increased and decreased ROS by hypoxia were documented as recently reviewed (33, 37, 38). The present study is consistent with those showing increased ROS by hypoxia (10, 26, 39–41). The oxidation of mitochondria-localized RoGFP observed here also suggests the origin of ROS, and this is generally consistent with the previous study showing increased oxidation of RoGFP in the intermembrane space but decreased oxidation of RoGFP in the mitochondrial matrix (40). H_2O_2 at the level achieved by hypoxia increased $[Ca^{2+}]_i$ in the presence of extracellular Ca^{2+}, which was diminished by the removal of extracellular Ca^{2+}, the presence of

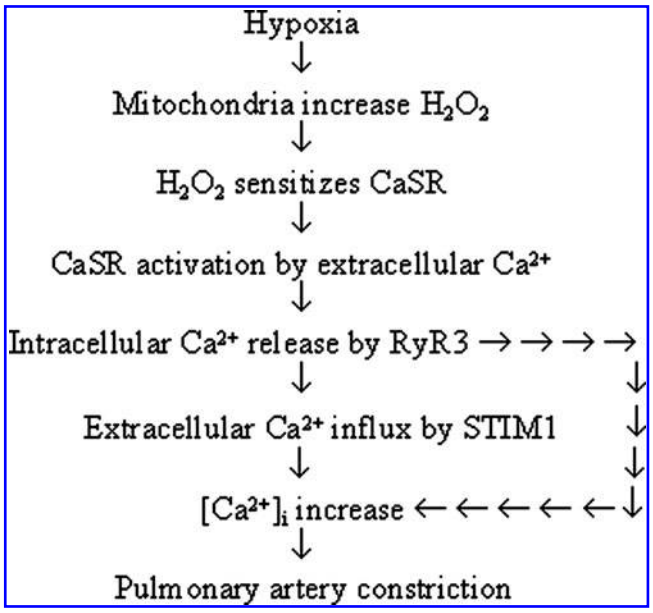

FIG. 10. The illustration of CaSR-mediated Ca^{2+} signaling in HPV.

Calhex231, or CaSR knockdown (Fig. 4). These results suggest that ROS elevated by hypoxia cannot directly stimulate intracellular Ca^{2+} release by itself and that H_2O_2 induces $[Ca^{2+}]_i$ elevation through CaSR in PASMCs. It also implies that the Ca^{2+} sensitivity of CaSR should be enhanced sufficiently by the H_2O_2 level or oxidized status achieved by hypoxia for mediating $[Ca^{2+}]_i$ elevation in the presence of constant extracellular Ca^{2+} level (without elevating $[Ca^{2+}]_o$ as the stimulus of CaSR). To better describe this process mechanistically, the present study adopts the expression of "sensing/sensitization," a concept usually used to indicate an altered activity of ion channel under oxidized/reduced status underlying HPV (33, 43) Thus, H_2O_2 at the level achieved by hypoxia induces $[Ca^{2+}]_i$ signaling in PASMCs through sensitizing CaSR. The mechanism underlying how hypoxia/ROS sensitizes CaSR remains unclear. One speculation can be the regulation of CaSR dimerization by disulfide bridge(s), although it is not an absolute requirement (2, 47).

The mitochondria-derived H_2O_2 was validated to sensitize CaSR and trigger HICI using mitochondria depletion strategy (Fig. 5). Ryanodine at the concentration inhibiting RyR or SOC inhibitor, but not IP_3 receptor inhibitor, significantly attenuated HICI (Fig. 6) that confirms previous reports (4, 8, 11, 15, 23, 34, 35, 48). An additional finding from the present study is that ryanodine/RyR3 knockdown and SOC inhibition/STIM1 knockdown similarly attenuated 15.6 μM HICI in PASMCs (Fig. 6), suggesting that RyR3 and STIM1 are likely the key components or downstream targets underlying CaSR activation or sensitization-triggered $[Ca^{2+}]_i$ signaling during hypoxia. In other words, the pivotal role of sensitized CaSR is to arrange or direct the mitochondria-derived H_2O_2, extracellular Ca^{2+}, the intracellular Ca^{2+} release pathway of RyR3, and the STIM1-participated extracellular Ca^{2+} influx pathway of SOC to orchestrate the $[Ca^{2+}]_i$ elevation during hypoxia in PASMCs. However, this study does not exclude the role of voltage-sensitive channels and myofilament Ca^{2+} sensitivity in HICI and HPV (1, 25, 28, 43). The inhibitory effect of ryanodine on HICI was swapped to XeC by the presence of a PKA inhibitor (Fig. 7), indicating that the switch of downstream target of CaSR activation from IP_3 receptor under normal/normoxic condition (14) to RyR under hypoxia is possibly related with PKA.

HPV is typically biphasic, an initial and transient one followed by a sustained constriction (4, 11, 16, 28, 29). The critical role of CaSR revealed in the current study appears applicable mainly to the initial phase and may also be involved in the sustained constriction (Supplementary Fig. S7).

Calhex231 and CaSR knockdown inhibited hypoxia-induced constriction of PA (Fig. 8). This is consistent with that CaSR activation in vascular smooth muscle cells can induce $[Ca^{2+}]_i$ elevation (17) and cause constriction of the gerbilline spiral modiolar artery (45) and that hypoxia- and peroxide-induced increase in $[Ca^{2+}]_i$ and contraction are intimately related in PASMCs (28, 29). Calhex231 also inhibited H_2O_2-induced PA constriction (Fig. 8), functionally confirming the signaling role of H_2O_2 in sensing CaSR, which, in turn, triggers PA constriction during hypoxia. The dose-dependent inhibition of HPV by Calhex231 was noted in rats, and the critical role of CaSR was further validated by the attenuated HPV in CaSR knockdown rats (Fig. 9). The effect of Calhex231 revealed in the current study appears to be specific, as it does not affect PE, high K^+, or angiotensionII-induced PA constriction (Supplementary Figs. S8 and S9). Taken together, these results provide functional evidence for the pivotal role of CaSR-mediated Ca^{2+} signaling in HPV, as illustrated in the mechanistic flow chart next (Fig. 10).

The blockage of hypoxia-triggered Ca^{2+} signaling in PASMCs by loading PEG-catalase and the essential role of CaSR in hypoxia-triggered Ca^{2+} signaling and HPV (Figs. 2–4, 5C, and 6–9) may warrant future studies to determine whether CaSR activity can be modulated by endogenous peroxidase and whether CaSR manipulation can potentially serve as a therapeutic target for HPV-related diseases such as hypoxic pulmonary hypertension and edema.

Materials and Methods

Cell culture

All experiments involving Sprague-Dawley rats were approved by the Institutional Animal Care and Use Committee.

Rat PASMCs were cultured from the third branches of intralobar artery explants and maintained in Dulbecco's modified Eagle's medium supplemented with 10% fetal bovine serum (7, 36). The PASMCs at ~70% confluence in 1–2 passages were employed in experiments. To deplete mitochondrial DNA, PASMCs were treated with 110 μg/ml sodium Py, 50 μg/ml Ur, and 200 ng/ml ethidium bromide as fully described earlier (7). PASMCs were isolated from at least three rats for each kind of experiment.

$[Ca^{2+}]_i$ measurement

$[Ca^{2+}]_i$ measurements were performed in 4-(2-hydroxyethyl)-1-piperazineethanesulfonic acid-buffered saline (HBS) containing (mM): NaCl 135, KCl 5.0, $CaCl_2$ 2.0, $MgSO_4$ 1.2, D-glucose 10, and HEPES 5 (pH 7.40) or without Ca^{2+} but with 1 mM ethylene glycol tetraacetic acid (EGTA) (0 $[Ca^{2+}]_o$) using Fura-2 as earlier (7, 49). For hypoxic stimulation, the HBS under normoxic condition in the bath was quickly

switched to hypoxic HBS through a sealed perfusion system. The hypoxic HBS was made ready before experiments by equilibration with and continuous bubbling of 100% N_2.

Intracellular ROS measurement

The detection of intracellular ROS using H_2DCFDA and its calibration exploiting the DCFDA oxidation speed *versus* extracellular application of a series of H_2O_2 were previously described in detail (7, 30, 49). The mitochondrial targeting RoGFP was generated from pAcGFP1-Mito vector (Clontech) by incorporating four mutations (C48S, Q80R, S147C, and Q204C) in GFP coding region (40) using a QuikChange Multi Site-directed mutagenesis kit (Stratagene), and the mutations were confirmed by sequencing. After transfection with Lipofectamine 2000, RoGFP images in PASMCs were obtained under a confocol microscope (OLYMPUS IX71) with excitation of 405 or 488 nm and emission at 515 ± 10 nm corresponding to the oxidized and reduced status, respectively. The ratios of fluorescence intensity from excitation at 405 and 488 nm were analyzed using FLUOVIEW V.5.0 software to quantify the extent of oxidative status.

Delivery of shRNA

Effective shRNA specifically against CaSR, STIM1, RyR3, and nonspecific control (Origene) were transfected into PASMCs using Lipofectamine 2000 as previously described (7). The shRNA constructs simultaneously encode GFP for identification of transfected PASMCs individually. The oligoDNA encoding the control and the effective shRNA targeting CaSR were subcloned into the Lenti-X shRNA expression vector (Clontech), respectively, confirmed by sequencing and packaged into lentiviral particles using Lenti-X HTX packaging system and 293T cells (Clonetech). 72 h before hemodynamic experiments, 1 ml lentivirus ($\sim 10^6$ TU/ml) was intravenously injected into each rat.

Immunochemical staining and western blot

To determine the expression of CaSR in PASMCs and endothelium-removed PAs, immunostaining and western blot were conducted as previously described in detail (7, 50) using an anti-CaSR antibody (Pierce Biotechnology).

Measurement of force

The endothelium-removed rings of intralobar PA were mounted in a wire myograph immersed in individual water-jacketed chambers containing physiological salt solution (118 NaCl, 24 $NaHCO_3$, 1 $MgSO_4$, 0.44 NaH_2PO_4, 4 KCl, 5.5 glucose, and 1.8 $CaCl_2$ mM, and pH 7.35–7.45), bubbled continuously with 95% O_2-5% CO_2 at 37°C, and stretched to a predetermined optimal passive tension of 500 mg. Force displacement was recorded using a PowerLab/4SP data acquisition system (ML118, AD Instruments). Each ring was initially contracted by 0.1 μM PE and subsequently challenged by 0.01 μM acetylcholine to confirm its contractility and endothelium nonintegrity, respectively. Since a small pretone by agonist can facilitate the hypoxic response in rat intralobar PA (16, 28), the rings were contracted by 0.1 μM PE 5 min before and during the hypoxic challenge. In some experiments, oxygen tension in the myograph chamber was simultaneously monitored *via* an isolated dissolved oxygen meter and electrode (ISO2, World Precision Instrument). Hypoxia was induced to a stable PO_2 level of 33 mmHg in PSS close to the rings within ~1.7 min by continuously bubbling with 95% N_2-5% CO_2.

Hemodynamic measurements

Rats were anesthetized with urethane (1.2 g/kg ip), and a catheter was inserted in the trachea and connected to a ventilator supplying room air or a 10% O_2-90% N_2 gas mixture. To continuously monitor pressure of pulmonary artery, a PE-50 tubing with a curved tip was passed from the right jugular vein into the main PA. The catheterization was also performed for the measurement of left ventricular end-diastolic pressure, and cardiac output (CO) was measured using the thermodilution method with the CO pod (ML313C, AD Instruments) and the PowerLab/4SP data acquisition system. A 200 μl of room temperature 0.9% NaCl solution was injected into the left jugular vein catheter with its tip near the right atrium, and changes in blood temperature were detected by a T-type ultra-fast thermocouple probe (MLT1402, Physitemp) positioned in the aortic arch from the right carotid artery.

Statistical analysis

Data are reported as means ± standard error. The Student's *t*-test and one-way analysis of variance analysis were made for two or multiple group comparisons, respectively. A difference was considered significant at $p < 0.05$.

Acknowledgments

The research was supported by 973 program-2012CB518201, NSFC grants (81170048, 30971162, 30670926 and 30770940), and a grant from key laboratory of high altitude medicine of MOE.

Author Disclosure Statement

No competing financial interests exist.

References

1. Archer SL, Wu XC, Thebaud B, Nsair A, Bonnet S, Tyrrell B, McMurtry MS, Hashimoto K, Harry G, and Michelakis ED. Preferential expression and function of voltage-gated, O_2-sensitive K^+ channels in resistance pulmonary arteries explains regional heterogeneity in hypoxic pulmonary vasoconstriction: ionic diversity in smooth muscle cells. *Circ Res* 95: 308–318, 2004.
2. Bai M, Trivedi S, and Brown EM. Dimerization of the extracellular calcium-sensing receptor (CaR) on the cell surface of CaR-transfected HEK293 cells. *J Biol Chem* 273: 23605–23610, 1998.
3. Bakhramov A, Evans AM, and Kozlowski RZ. Differential effects of hypoxia on the intracellular Ca^{2+} concentration of myocytes isolated from different regions of the rat pulmonary arterial tree. *Exp Physiol* 83: 337–347, 1998.
4. Becker S, Knock GA, Snetkov V, Ward JP, and Aaronson PI. Role of capacitative Ca^{2+} entry but not Na^+/Ca^{2+} exchange in hypoxic pulmonary vasoconstriction in rat intrapulmonary arteries. *Novartis Found Symp* 272: 259–268; discussion 268–279, 2006.
5. Brown EM, Gamba G, Riccardi D, Lombardi M, Butters R, Kifor O, Sun A, Hediger MA, Lytton J, and Hebert SC.

Cloning and characterization of an extracellular Ca^{2+}-sensing receptor from bovine parathyroid. *Nature* 366: 575–580, 1993.
6. Chattopadhyay N, Cheng I, Rogers K, Riccardi D, Hall A, Diaz R, Hebert SC, Soybel DI, and Brown EM. Identification and localization of extracellular Ca^{2+}-sensing receptor in rat intestine. *Am J Physiol* 274: G122–G130, 1998.
7. Chen T, Zhu L, Wang T, Ye H, Huang K, and Hu Q. Mitochondria depletion abolishes agonist-induced Ca^{2+} plateau in airway smooth muscle cells: potential role of H_2O_2. *Am J Physiol Lung Cell Mol Physiol* 298: L178–L188, 2010.
8. Cornfield DN, Stevens T, McMurtry IF, Abman SH, and Rodman DM. Acute hypoxia causes membrane depolarization and calcium influx in fetal pulmonary artery smooth muscle cells. *Am J Physiol* 266: L469–L475, 1994.
9. Cornfield DN, Stevens T, McMurtry IF, Abman SH, and Rodman DM. Acute hypoxia increases cytosolic calcium in fetal pulmonary artery smooth muscle cells. *Am J Physiol* 265: L53–L56, 1993.
10. Desireddi JR, Farrow KN, Marks JD, Waypa GB, and Schumacker PT. Hypoxia increases ROS signaling and cytosolic Ca^{2+} in pulmonary artery smooth muscle cells of mouse lungs slices. *Antioxid Redox Signal* 12: 595–602, 2010.
11. Du W, Frazier M, McMahon TJ, and Eu JP. Redox activation of intracellular calcium release channels (ryanodine receptors) in the sustained phase of hypoxia-induced pulmonary vasoconstriction. *Chest* 128: 556S–558S, 2005.
12. Gelband CH and Gelband H. Ca^{2+} release from intracellular stores is an initial step in hypoxic pulmonary vasoconstriction of rat pulmonary artery resistance vessels. *Circulation* 96: 3647–3654, 1997.
13. Harder DR, Madden JA, and Dawson C. Hypoxic induction of Ca^{2+}-dependent action potentials in small pulmonary arteries of the cat. *J Appl Physiol* 59: 1389–1393, 1985.
14. Hofer AM and Brown EM. Extracellular calcium sensing and signalling. *Nat Rev Mol Cell Biol* 4: 530–538, 2003.
15. Jabr RI, Toland H, Gelband CH, Wang XX, and Hume JR. Prominent role of intracellular Ca^{2+} release in hypoxic vasoconstriction of canine pulmonary artery. *Br J Pharmacol* 122: 21–30, 1997.
16. Leach RM, Hill HM, Snetkov VA, Robertson TP, and Ward JP. Divergent roles of glycolysis and the mitochondrial electron transport chain in hypoxic pulmonary vasoconstriction of the rat: identity of the hypoxic sensor. *J Physiol* 536: 211–224, 2001.
17. Li GW, Wang QS, Hao JH, Xing WJ, Guo J, Li HZ, Bai SZ, Li HX, Zhang WH, Yang BF, Yang GD, Wu LY, Wang R, and Xu CQ. The functional expression of extracellular calcium-sensing receptor in rat pulmonary artery smooth muscle cells. *J Biomed Sci* 18: 16, 2010.
18. Lin MJ, Yang XR, Cao YN, and Sham JS. Hydrogen peroxide-induced Ca^{2+} mobilization in pulmonary arterial smooth muscle cells. *Am J Physiol Lung Cell Mol Physiol* 292: L1598–L1608, 2007.
19. Liu Q, Sham JS, Shimoda LA, and Sylvester JT. Hypoxic constriction of porcine distal pulmonary arteries: endothelium and endothelin dependence. *Am J Physiol Lung Cell Mol Physiol* 280: L856–L865, 2001.
20. Mauban JR, Remillard CV, and Yuan JX. Hypoxic pulmonary vasoconstriction: role of ion channels. *J Appl Physiol* 98: 415–420, 2005.
21. Molostvov G, Fletcher S, Bland R, and Zehnder D. Extracellular calcium-sensing receptor mediated signalling is involved in human vascular smooth muscle cell proliferation and apoptosis. *Cell Physiol Biochem* 22: 413–422, 2008.
22. Ng LC, Kyle BD, Lennox AR, Shen XM, Hatton WJ, and Hume JR. Cell culture alters Ca^{2+} entry pathways activated by store-depletion or hypoxia in canine pulmonary arterial smooth muscle cells. *Am J Physiol Cell Physiol* 294: C313–C323, 2008.
23. Ng LC, Wilson SM, and Hume JR. Mobilization of sarcoplasmic reticulum stores by hypoxia leads to consequent activation of capacitative Ca^{2+} entry in isolated canine pulmonary arterial smooth muscle cells. *J Physiol* 563: 409–419, 2005.
24. Oda Y, Tu CL, Pillai S, and Bikle DD. The calcium sensing receptor and its alternatively spliced form in keratinocyte differentiation. *J Biol Chem* 273: 23344–23352, 1998.
25. Olschewski A, Hong Z, Nelson DP, and Weir EK. Graded response of K^+ current, membrane potential, and $[Ca^{2+}]_i$ to hypoxia in pulmonary arterial smooth muscle. *Am J Physiol Lung Cell Mol Physiol* 283: L1143–L1150, 2002.
26. Paddenberg R, Ishaq B, Goldenberg A, Faulhammer P, Rose F, Weissmann N, Braun-Dullaeus RC, and Kummer W. Essential role of complex II of the respiratory chain in hypoxia-induced ROS generation in the pulmonary vasculature. *Am J Physiol Lung Cell Mol Physiol* 284: L710–L719, 2003.
27. Platoshyn O, Yu Y, Ko EA, Remillard CV, and Yuan JX. Heterogeneity of hypoxia-mediated decrease in IK_V and increase in $[Ca^{2+}]_{cyt}$ in pulmonary artery smooth muscle cells. *Am J Physiol Lung Cell Mol Physiol* 293: L402–L416, 2007.
28. Robertson TP, Aaronson PI, and Ward JP. Hypoxic vasoconstriction and intracellular Ca^{2+} in pulmonary arteries: evidence for PKC-independent Ca^{2+} sensitization. *Am J Physiol* 268: H301–H307, 1995.
29. Robertson TP, Hague D, Aaronson PI, and Ward JP. Voltage-independent calcium entry in hypoxic pulmonary vasoconstriction of intrapulmonary arteries of the rat. *J Physiol* 525(Pt 3): 669–680, 2000.
30. Roy S, Parinandi N, Zeigelstein R, Hu Q, Pei Y, Travers JB, and Natarajan V. Hyperoxia alters phorbol ester-induced phospholipase D activation in bovine lung microvascular endothelial cells. *Antioxid Redox Signal* 5: 217–228, 2003.
31. Rueda A, Song M, Toro L, Stefani E, and Valdivia HH. Sorcin modulation of Ca^{2+} sparks in rat vascular smooth muscle cells. *J Physiol* 576: 887–901, 2006.
32. Russell MJ, Pelaez NJ, Packer CS, Forster ME, and Olson KR. Intracellular and extracellular calcium utilization during hypoxic vasoconstriction of cyclostome aortas. *Am J Physiol Regul Integr Comp Physiol* 281: R1506–R1513, 2001.
33. Sommer N, Dietrich A, Schermuly RT, Ghofrani HA, Gudermann T, Schulz R, Seeger W, Grimminger F, and Weissmann N. Regulation of hypoxic pulmonary vasoconstriction: basic mechanisms. *Eur Respir J* 32: 1639–1651, 2008.
34. Vadula MS, Kleinman JG, and Madden JA. Effect of hypoxia and norepinephrine on cytoplasmic free Ca^{2+} in pulmonary and cerebral arterial myocytes. *Am J Physiol* 265: L591–L597, 1993.
35. Wang J, Shimoda LA, Weigand L, Wang W, Sun D, and Sylvester JT. Acute hypoxia increases intracellular $[Ca^{2+}]$ in pulmonary arterial smooth muscle by enhancing capacitative Ca^{2+} entry. *Am J Physiol Lung Cell Mol Physiol* 288: L1059–L1069, 2005.
36. Wang T, Zhang ZX, Xu YJ, and Hu QH. 5-Hydroxydecanoate inhibits proliferation of hypoxic human pulmonary artery

smooth muscle cells by blocking mitochondrial K_{ATP} channels. *Acta Pharmacol Sin* 28: 1531–1540, 2007.
37. Wang YX and Zheng YM. ROS-dependent signaling mechanisms for hypoxic Ca^{2+} responses in pulmonary artery myocytes. *Antioxid Redox Signal* 12: 611–623, 2010.
38. Ward JP and McMurtry IF. Mechanisms of hypoxic pulmonary vasoconstriction and their roles in pulmonary hypertension: new findings for an old problem. *Curr Opin Pharmacol* 9: 287–296, 2009.
39. Waypa GB, Chandel NS, and Schumacker PT. Model for hypoxic pulmonary vasoconstriction involving mitochondrial oxygen sensing. *Circ Res* 88: 1259–1266, 2001.
40. Waypa GB, Marks JD, Guzy R, Mungai PT, Schriewer J, Dokic D, and Schumacker PT. Hypoxia triggers subcellular compartmental redox signaling in vascular smooth muscle cells. *Circ Res* 106: 526–535, 2010.
41. Waypa GB, Marks JD, Mack MM, Boriboun C, Mungai PT, and Schumacker PT. Mitochondrial reactive oxygen species trigger calcium increases during hypoxia in pulmonary arterial myocytes. *Circ Res* 91: 719–726, 2002.
42. Weigand L, Foxson J, Wang J, Shimoda LA, and Sylvester JT. Inhibition of hypoxic pulmonary vasoconstriction by antagonists of store-operated Ca^{2+} and nonselective cation channels. *Am J Physiol Lung Cell Mol Physiol* 289: L5–L13, 2005.
43. Weir EK, Cabrera JA, Mahapatra S, Peterson DA, and Hong Z. The role of ion channels in hypoxic pulmonary vasoconstriction. *Adv Exp Med Biol* 661: 3–14, 2010.
44. Weissberg PL, Little PJ, and Bobik A. Spontaneous oscillations in cytoplasmic calcium concentration in vascular smooth muscle. *Am J Physiol* 256: C951–C957, 1989.
45. Wonneberger K, Scofield MA, and Wangemann P. Evidence for a calcium-sensing receptor in the vascular smooth muscle cells of the spiral modiolar artery. *J Membr Biol* 175: 203–212, 2000.
46. Yang ZW, Zheng T, Wang J, Zhang A, Altura BT, and Altura BM. Hydrogen peroxide induces contraction and raises $[Ca^{2+}]_i$ in canine cerebral arterial smooth muscle: participation of cellular signaling pathways. *Naunyn Schmiedebergs Arch Pharmacol* 360: 646–653, 1999.
47. Zhang Z, Sun S, Quinn SJ, Brown EM, and Bai M. The extracellular calcium-sensing receptor dimerizes through multiple types of intermolecular interactions. *J Biol Chem* 276: 5316–5322, 2001.
48. Zheng YM, Wang QS, Rathore R, Zhang WH, Mazurkiewicz JE, Sorrentino V, Singer HA, Kotlikoff MI, and Wang YX. Type-3 ryanodine receptors mediate hypoxia-, but not neurotransmitter-induced calcium release and contraction in pulmonary artery smooth muscle cells. *J Gen Physiol* 125: 427–440, 2005.
49. Zhu L, Luo Y, Chen T, Chen F, Wang T, and Hu Q. Ca^{2+} oscillation frequency regulates agonist-stimulated gene expression in vascular endothelial cells. *J Cell Sci* 121: 2511–2518, 2008.
50. Ziegelstein RC, Xiong Y, He C, and Hu Q. Expression of a functional extracellular calcium-sensing receptor in human aortic endothelial cells. *Biochem Biophys Res Commun* 342: 153–163, 2006.

Address correspondence to:
Dr. Qinghua Hu
Department of Pathophysiology
Tongji Medical College
Huazhong University of Science and Technology (HUST)
Wuhan 430030
People's Republic of China

E-mail: qinghuaa@mails.tjmu.edu.cn

Date of first submission to ARS Central, July 18, 2011; date of final revised submission, November 18, 2011; date of acceptance, November 18, 2011.

Abbreviations Used

Ach = acetylcholine
$[Ca^{2+}]_i$ = cytosolic calcium
CaSR = calcium-sensing receptor
CO = cardiac output
DCFDA = 2′, 7′-dichlorofluorescin diacetate
EGTA = ethylene glycol tetraacetic acid
GFP = green fluorescent protein
HEPES = 4-(2-hydroxyethyl)-1-piperazineethanesulfonic acid
HICI = hypoxia-induced $[Ca^{2+}]_i$ increase
HPV = hypoxic pulmonary vasoconstriction
KPSS = KCl-physiological salt solution
LVEDP = left ventricular end-diastolic pressure
NS = nonsignificance
PA = pulmonary artery
PASMCs = pulmonary artery smooth muscle cells
PE = phenylephrine
PEG = polyethylene glycol
PKA = protein kinase A
Ppa = pressure of pulmonary artery
ROS = reactive oxygen species
RyRs = ryanodine receptors
SOC = store-operated Ca^{2+} influx